# THERMAL-HYDRAULIC MODELLING AND ANALYSIS OF A SMALL MODULAR REACTOR

SALAH EL-DIN EL-MORSHEDY
Egyptian Atomic Energy Authority
Cairo, Egypt
Email: s.e.elmorshedy@gmail.com

**Abstract**

A mathematical model has been developed to simulate the thermal-hydraulic performance for a near term deployable SMR of the integral pressurized water reactor (IPWR) design under normal operation. The energy equation and the heat conduction equation are solved analytically in order to predict the coolant, clad and fuel temperature distributions. The core active length is divided into axial regions and the fuel rod is divided into radial zones, nodal calculation is performed for two types of cooling channels; the average and the hot channels. Through this model, the heat flux leading to the Departure from Nucleate Boiling (DNB) as well as the Departure from Nucleate Boiling Ratio (DNBR) predicted at each axial node for each channel using EPRI correlation. High accuracy correlations and/or models valid under the reactor operating conditions are selected to estimate the heat transfer coefficients under single-phase forced convection, subcooled boiling and bulk boiling regimes. The vapor quality and void fraction are estimated for boiling regimes as well. The model is then used to simulate the reactor performance under different core cooling flow rates ranging from 10000 to 18000 $m^3/h$ and so different subcooling margins. The developed model can be used for selecting the appropriate core flow rate and subcooling margin and performing independent thermal-hydraulic safety assessment of the reactor core under steady-state operation as well.

## 1. INTRODUCTION

The study of small modular reactors has generated increasing interest in recent years in the international scientific community. Their applications and versatility make them an attractive option among candidates considered in generation III+ and IV. Erfaninia et al. [1] presented a neutronic-thermal hydraulics coupling analysis of the fuel channel of an advanced Small Modular Reactor (SMR), which is nominated as a near term option of the generation IV reactors. They choose CAREM25 as the reference SMR. Yu et al. [2] analyzed neutron physics and thermal hydraulics for SMR loaded with ATFs. Their results show that the 4% uranium enriched ATF pellets can meet the lifetime requirements, and the application of silicon uranium fuel pellets can significantly reduce maximum fuel centerline temperature (MFCT). Zhao et al. [3] developed a thermal-hydraulic analysis code for small modular natural circulation LFRs, which is based on several mathematical models for natural circulation originally. Kim and Jeong [4] developed a detailed CFD simulation analysis model using ANSYS CFX 16.1 to simulate the basic design and internal flow characteristics of a 180 MW SMR with a natural circulation flow system. The K-factor was calculated from the flow analysis data of the CFX model and applied to an analysis model in RELAP5/MOD3.3. The CFX analysis results and RELAP analysis results were evaluated in terms of the internal flow characteristics per core output. Kitcher and Chirayath [5] developed a physics model of a near term deployable SMR of the integral pressurized water reactor (IPWR) design. They performed fuel depletion simulations to optimize the active fuel length, fuel enrichment and core loading pattern in order to achieve a uniform core power distribution. Their optimized core can produce 500 MW of thermal power with a four year core life-time at a capacity factor of 87%. The core consists of 69 uranium dioxide ($UO_2$) fuel assemblies; 5 assemblies at 4.4% $^{235}U$ enrichment and 64 assemblies at 4.95% $^{235}U$ enrichment. The active fuel length is 200 cm and the core diameter is 194.55 cm for an active core height-to-diameter ratio of 1.03. In the present work, a thermal-hydraulic model is developed to simulate the thermal-hydraulic performance for a near term deployable SMR of the integral pressurized water reactor (IPWR) design [5] under different core cooling flow rates ranging from 10000 to 18000 $m^3/h$ and so different subcooling margins. The SMR fuel assemblies are to be exactly the same as the typical existing large PWR with respect to materials and dimensions except for the active fuel length. As such a typical 17x17 fuel assembly configuration was chosen. The fuel assembly parameters used in the model was kept the same as the existing large PWR. Table 1 presents the reactor main parameters

TABLE 1 SMR MAIN PARAMETERS

| Parameter | Value |
|---|---|
| Reactor power (MWt) | 500 |
| Core pressure (MPa) | 15 |
| Core inlet temperature (°C) | 288 |
| Axial peaking factor | 1.09 |
| Radial peaking factor | 1.24 |
| Active fuel length (cm) | 200 |
| Pellet diameter (cm) | 0.784 |
| Gap outer diameter (cm) | 0.816 |
| Clad outer diameter (cm) | 0.93 |
| Fuel lattice pitch (cm) | 1.26 |
| Number of fuel assemblies | 69 |
| Assembly size | 17x17 |
| Fuel rods per assembly | 264 |

## 2. MATHEMATICAL MODEL

Two types of coolant channels are selected for modelling the reactor core; one channel representing the core average channel and the other channel representing the hot channel. Each coolant channel is divided into axial regions while the fuel rod is divided into radial nodes, and then a nodal calculation is performed.
The axial heat flux distribution along the core is considered cosine shape.

$$\phi(z) = \phi_0 \cos\left(\frac{\pi(z - L/2)}{L}\right) \tag{1}$$

where $\phi_0$ is the maximum axial heat flux and is given by:

for the average channel $$\phi_0\big|_a = RPF \times \phi_{av} \tag{2}$$

for the hot channel $$\phi_0\big|_h = APF \times RPF \times \phi_{av} \tag{3}$$

where $L$ is the fuel length and $RPF$ and $APF$ are is the radial and axial peaking factors respectively.

### 2.1. Coolant temperature

As the coolant moves along the fuel, it absorbs heat, and, as a result, its temperature continually increases. In order to calculate the bulk coolant temperature at a height 'z' from the channel inlet, the general energy balance equation is applied on each control volume of the coolant channel.

$$I_b(i) = I_b(i-1) + 2 \times \frac{[\phi(I) + \phi(I-1)]D\,\Delta Z}{G\,D_e^2} \tag{4}$$

### 2.2. Clad and fuel temperatures

The steady-state temperature distribution through the fuel rod is determined by solving the heat conduction equation in cylindrical coordinates for both the clad and fuel regions analytically as follows:

$$\frac{1}{r}\frac{\partial}{\partial r}\left(kr\frac{\partial T}{\partial r}\right) + q = 0 \tag{5}$$

*Clad-outer-surface temperature* $$T_{co}(i) = T_b(i) + \frac{\phi(i)}{h(i)} \tag{6}$$

*Clad-inner-surface temperature* $$T_{ci}(i) = T_{co}(i) - \frac{\phi(i)\,D}{2k_c}\ln\left(\frac{D_{ci}}{D}\right) \tag{7}$$

*Fuel-outer-surface temperature* $$T_{fo}(i) = T_{ci}(i) + \frac{\phi(i)}{h_g} \times \frac{2D}{D_{ci} + D_{fo}} \tag{8}$$

where $h_g$ is the gap conductance of the fuel-clad gap that is predicted as follows:

$$h_g = h_{open} + h_{contact} \tag{9}$$

The conductance across the gap is considered as the sum of heat transfer across the open gap ($h_{open}$) and heat transfer coefficient for gap closure ($h_{contact}$) occurs because of fuel swelling and thermal expansion. The heat transfer coefficient for open gap is obtained by:

$$h_{open} = \frac{k_g}{\delta_{eff}} + \frac{\sigma}{\frac{1}{\varepsilon_c} + \frac{1}{\varepsilon_f} - 1} \times \frac{T_{fo}(i)^4 - T_{ci}(i)^4}{T_{fo}(i) - T_{ci}(i)} \tag{10}$$

where $k_g$ is the thermal conductivity of the gas, $\delta_{eff}$ is the effective gap width, $\sigma$ is Stefan-Boltzmann constant; $\varepsilon_f$ is the surface emissivity of the fuel and $\varepsilon_c$ is the surface emissivity of the clad. The effective gap width can be calculated as:

$$\delta_{eff} = \delta_g + \delta_{jump} \tag{11}$$

where $\delta_g$ is gap width and $\delta_{jump}$ is found to be 10 μm in helium. The gas conductivity of a pure gas is given by:

$$k_g = A \times 10^{-4} T_g^{0.79} \tag{12}$$

where $A$ is 15.8 for helium and $T_g$ is the gas temperature. The contact-related heat transfer coefficient that is proportional to the surface contact pressure can be given by [6]:

$$h_{contact} = C \times \frac{2 k_f \, k_c}{k_f + k_c} \times \frac{P_i}{H \sqrt{\delta_g}} \tag{13}$$

where $C$ is a constant (= 10 ft$^{-1/2}$), $p_i$ is surface contact pressure in psi, $H$ is Meyer's hardness number that is $14 \times 10^4$ psi for zircaloy cladding and $k_f$ is the fuel thermal conductivity.

*Fuel-inner-surface temperature*

$$T_{fi}(i) = T_{fo}(i) + \frac{\phi(i)\, D}{4 k_f} \tag{14}$$

## 2.3. Coefficient of Heat Transfer

The heat transfer coefficient is calculated for the water coolant under single-phase liquid or boiling two-phase flow condition where the heat transfer coefficient is obtained as follows:

### *2.3.1. Single-phase liquid forced convection*

The coolant flow through the reactor core is water flowing through a lattice of rods is obtained by:

$$Nu = C \, \mathrm{Re}^m \, \mathrm{Pr}^n \tag{15}$$

where the recommended constants are: $m$ = 0.8, $n$ = 1 /3 , and $C$ is given by:

$$C = 0.042 \times \frac{S}{D} - 0.024 \tag{16}$$

for square lattices with $1.1 \leq \frac{S}{D} \leq 1.3$, the quantities $S$ and $D$ are the lattice pitch and rod diameter respectively.

### *2.3.2. Subcooled boiling*

Boiling is commenced when the clad-outer-surface temperature is equal to or exceed the onset of nucleate boiling temperature, $T_{ONB}$, where

$$T_{ONB} = T_{sat} + (\Delta T_{sat})_{ONB} \tag{17}$$

Frost and Dzakowic [8] correlation is used in the present model as:

$$(\Delta T_{sat})_{ONB} = \left( \frac{8 \sigma \phi T_{sat}}{k_l \, I_{fg} \, \rho_g} \right)^{0.5} \mathrm{Pr}_l \tag{18}$$

The correlation developed by Thom et al. [9] is used in the subcooled boiling regime as:

$$\Delta T_{sat} = 0.072 \phi^{0.5} \, e^{-P/1260} \tag{19}$$

### *2.3.3. Saturated nucleate boiling*

The heat transfer coefficient in forced flow saturated boiling is obtained by the Steiner-Taborek [10] asymptotic model. Steiner-Taborek model combines the effects of convection and nucleate boiling as follows:

$$h_{TP} = \left[ (h_{SP} . F_{TP})^3 + (h_{NCB} . F_{NCB})^3 \right]^{1/3} \tag{20}$$

where the single-phase liquid heat transfer coefficient, $h_{SP}$ is given by Gnielinski correlation as:

$$h_{SP} = \left(\frac{k_l}{D_e}\right)\left(\frac{(f/8)(\mathrm{Re}-1000)\mathrm{Pr}}{1+12.7(f/8)^{1/2}\left(\mathrm{Pr}^{2/3}-1\right)}\right) \tag{21}$$

where the Fanning friction factor, $f$ is obtained from:

$$f = \left[0.7904\ln(\mathrm{Re}) - 1.64\right]^{-2} \tag{22}$$

and is valid for 4000 < Re < 5000000 and 0.5 < Pr < 2000

The two-phase multiplier, $F_{TP}$ is given by:

$$F_{TP} = \left[(1-x)^{1.5} + 1.9\,x^{0.6}\left(\rho_l/\rho_g\right)^{0.35}\right]^{1.1} \tag{23}$$

where $x$ is the steam quality.

In this method, the nucleate pool boiling coefficient $h_{NCB}$ is the nucleate flow boiling coefficient at the standard conditions of reduced pressure $P_r$ = 0.1, mean surface roughness, $R_{po}$ = 1 μm, tube diameter, $D_o$ = 0.01 m and the heat flux, $\phi_o$ = 150000 W. This coefficient is equal to 25580 W/m$^2$ $^o$C.

The nucleate boiling correction factor is given by:

$$F_{NCB} = F_{PF}\left(\frac{\phi}{\phi_o}\right)^{nf}\left(\frac{D_e}{D_o}\right)^{-0.4}\left(\frac{R_p}{R_{po}}\right)^{0.133} F(M) \tag{24}$$

where the pressure correction factor, $F_{PF}$ valid for $P_r$ < 0.95 is:

$$F_{PF} = 2.816\,P_r^{045} + \left(3.4 + \frac{1.7}{1-P_r^7}\right)P_r^{3.7} \tag{25}$$

and the exponent, $nf$ is given by:

$$nf = 0.8 - 0.1\times\exp(1.75\,P_r) \tag{26}$$

The residual correction factor, *F(M)* is a function of liquid molecular weight $M$ as:

$$F(M) = 0.377 + 0.99\ln(M) + 0.000028427 \tag{27}$$

## 2.4. Critical heat flux

EPRI correlation is used in the present model to calculate the critical heat flux as follows:

$$\phi_{CHF}\left(\frac{BTU}{ft^2 hr}\right) = \frac{A\,F_A - x_{in}}{C\,F_C\,F_g F_{nu} + \left(\dfrac{x - x_{in}}{\phi}\right)} \tag{37}$$

with $A = 0.5328 P_r^{0.1212}\,G^{(-0.3040-0.3285 P_r)}$ and $C = 1.6151 P_r^{1.4066}\,G^{(0.4843-2.0749 P_r)}$

$F_A$, $F_C$, $F_g$ and $F_{nu}$ are optional factors which correct the critical heat flux for various effects; otherwise they are assigned to the value of 1.0. If non-uniform axial profile: $F_{nu} = 1 + \frac{1-Y}{1+G}$ $\quad where\ Y = \frac{1}{L}\int_0^L \frac{\phi(z)}{\phi_{local}}dz$; else $F_{nu}$ = 1.0

## 3. RESULTS AND DISCUSSION

Calculations are performed for the beginning of life of the reactor under steady-state operation. The reactor core is modelled in two types of channels; the average and hot channels. The coolant channels are divided into 50 axial regions and the fuel rod is divided into 10 radial nodes (7 for fuel zone and 3 for clad zone). The steady-state coolant bulk temperature profile is plotted in Fig. 3 for both the average and hot channels under different core cooling flow rates ranging from 10000 to 18000 m3/h and so different subcooling margins. It shows that, the coolant is always subcooled under this range of coolant flow-rate. Fig. 2 shows the clad-outer-surface temperature profiles for the fuel rod of both the average and hot channel under core cooling flow rates ranging from 10000 to 18000 m$^3$/h. It shows that the clad-outer-surface temperature exceeds the ONB temperature and so subcooled boiling is achieved for the core flow-rate less than 13000 m$^3$/h in the average channel and in the hot channel for the core flow-rate less than or equal to 13000 m$^3$/h. It is noticed that, the predicted clad-outer-surface-temperature remains below 350$^o$C. In order to avoid boiling phenomenon at the cladding surface; it is recommended to adapt a core cooling flow rate greater than or equal to13000 m$^3$/h. Fig. 3 shows the fuel-center temperature profile for the fuel rod of both the average and hot channel under the aforementioned range of core cooling flow-rate. The maximum fuel temperature values predicted are less than 1210$^o$C. Fig. 4 shows the distribution of the predicted DNBR along the hottest fuel rod for all cases. It is found that the minimum DNBR values ranges from 1.55 for core flow-rate of 10000 m$^3$/h to 2.38 for core flow-rate of

18000 $m^3$/h. Fig. 4 shows also the subcooling margins for core cooling flow rates ranging from 10000 to 18000 $m^3$/h. It shows that, the subcooling margin is 9$^o$C for core cooling flow-rate of 10000 $m^3$/h and increases by increasing the core cooling flow-rate to reach 27$^o$C at core cooling flow-rate of 18000 $m^3$/h.

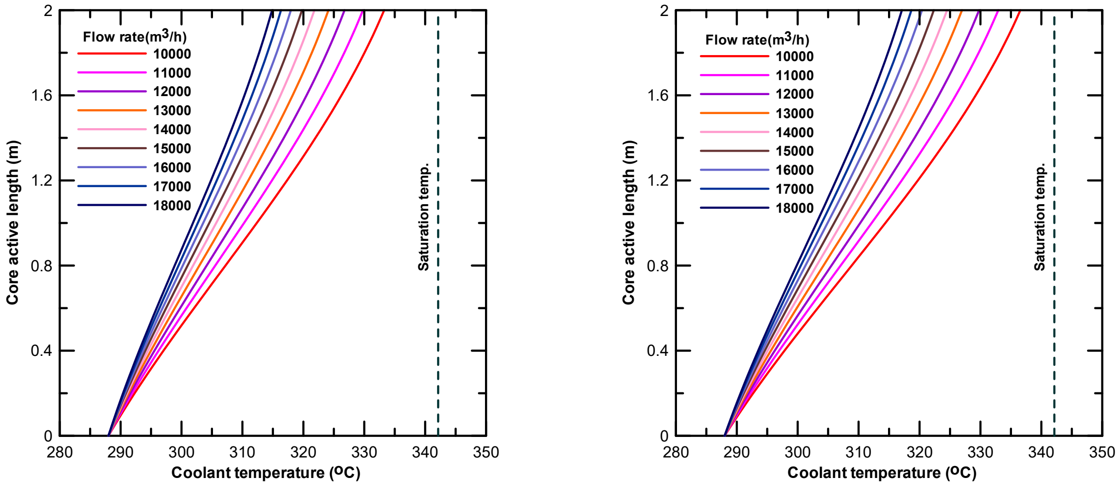


(a) (b)

*FIG. 1. Coolant temperature profile: (a) average channel and (b) hot channel.*

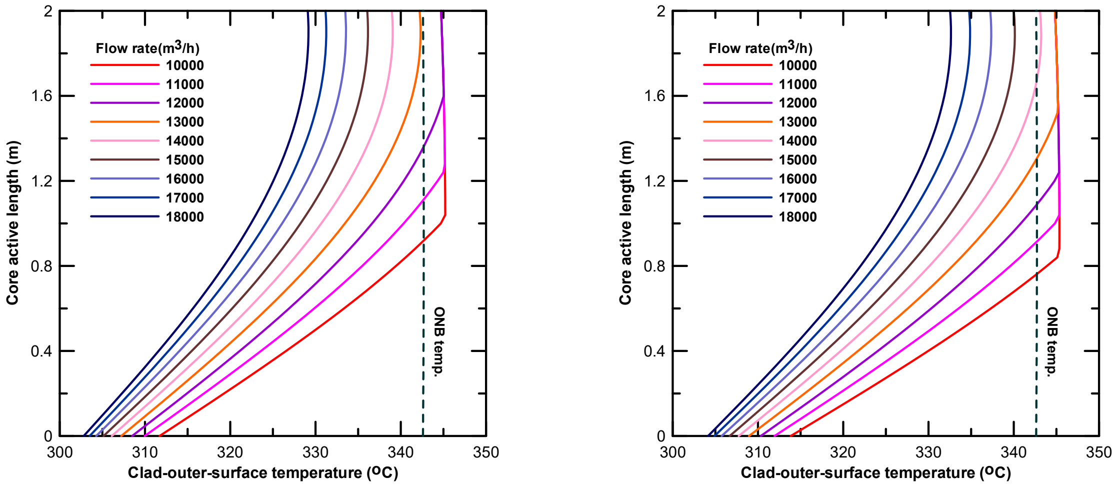


(a) (b)

*FIG. 2. Clad-outer-surface temperature profile: (a) average channel and (b) hot channel.*

## 4. CONCLUSIONS

A mathematical model to simulate the thermal-hydraulic behavior of SMR of the integral pressurized water reactor (IPWR) design during normal operation has been developed. The model has the ability to simulate the core average and hot channels. The coolant temperature is determined through a simple heat balance. The heat conduction equation is solved analytically in cylindrical coordinates to obtain the temperature distribution through the fuel and cladding materials. Besides, the critical heat flux is determined and the departure from nucleate boiling ratio which measures the safety margin for burnout is predicted. The heat transfer correlations and/or models implemented in the model are selected to be valid under the reactor operating conditions with a high accuracy. The vapor quality and void fraction are evaluated for boiling regimes as well. The model is used to simulate the reactor performance under different core cooling flow rates ranging from 10000 to 18000 $m^3$/h and so different subcooling margins. It is found that, subcooled boiling is predicted for core cooling flow-rate less than or equal 13000 $m^3$/h. Therefore; in order to avoid boiling it is recommended to a core cooling flow-rate greater than 13000 $m^3$/h resulting in a subcooling margin higher than 18$^o$C. It is found that the minimum DNBR values ranges from 1.55 for core flow-rate of 10000 $m^3$/h to 2.38 for core flow-rate of 18000 $m^3$/h.

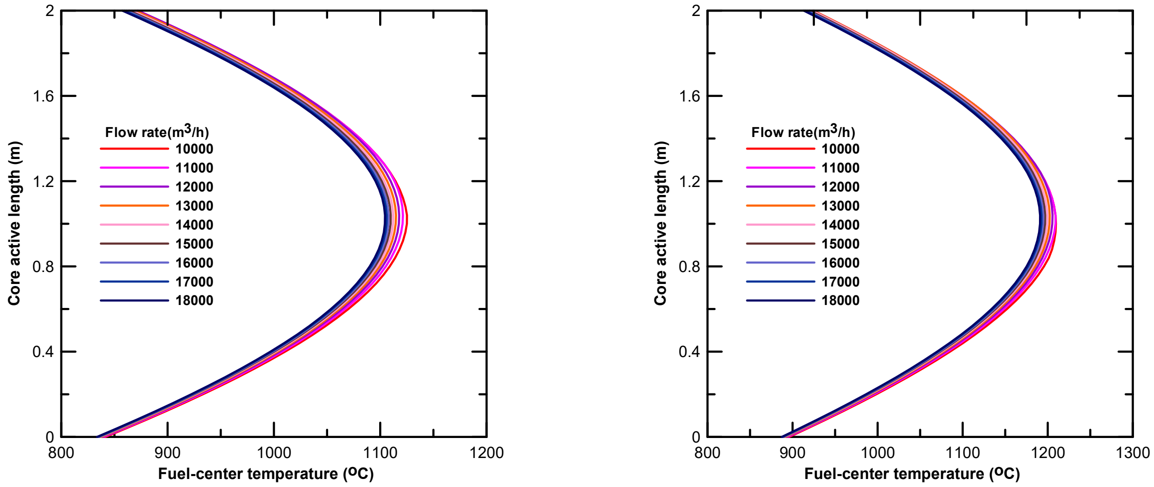


(a) (b)

*FIG. 3. Fuel-center temperature profile: (a) average channel and (b) hot channel.*

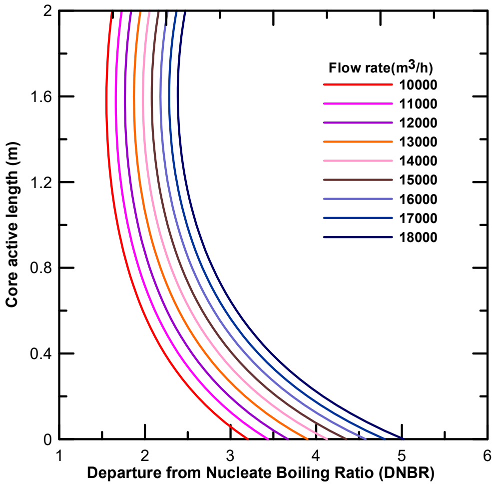


*FIG. 4. CHF and DNBR along the hottest fuel rod.*

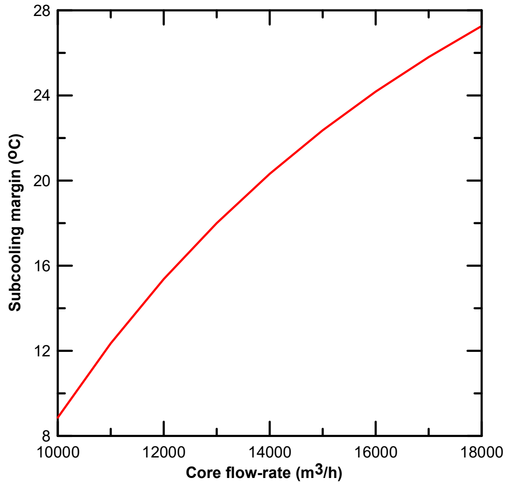


*FIG. 5. Subcooling margin.*

## REFERENCES

[1] Ali Erfaninia, Afshin Hedayat, S.M. Mirvakili and M.R. Nematollahi, Neutronic-thermal hydraulic coupling analysis of the fuel channel of a new generation of the small modular pressurized water reactor including hexagonal and square fuel assemblies using MCNP and CFX, Progress in Nuclear Energy, 2017, Pages 213-227.

[2] Honghao Yu, Jiejin Cai, Sihong He and Xuezhong Li, Analysis of neutron physics and thermal hydraulics for fuel assembly of small modular reactor loaded with ATFs, Annals of Nuclear Energy, Volume 152, 2021, 107957.

[3] Pengcheng Zhao, Zijing Liu, Tao Yu, Jinsen Xie, Zhenping Chen and Chong Shen, Code development on steady-state thermal-hydraulic for small modular natural circulation lead-based fast reactor, Nuclear Engineering and Technology, Volume 52, Issue 12, December 2020, Pages 2789-2802.

[4] Mun Soo Kim and Yong Hoon Jeong, Conceptual design of small modular reactor driven by natural circulation and study of design characteristics using CFD & RELAP5 code, Nuclear Engineering and Technology, 2020.

[5] Evans D. Kitcher and Sunil S. Chirayath, Neutronics and thermal hydraulics analysis of a small modular reactor, Annals of Nuclear Energy, Volume 97, November 2016, Pages 232-245.

[6] W. Frost and G. S. Dzakowic, An extension of the method of predictive incipient boiling on commercially finished surfaces, in: ASME-AIChE Heat Transfer Conference, Seattle, 1967.

[7] J. R. S. Thorn, W. M. Walker, T. A. Fallon and G. F. S. Reising, Boiling in subcooled water during flow up heated tubes or annuli, Paper 6 presented at the Symposium on Boiling Heat Transfer in Steam Generation Units and Heat Exchangers held in Manchester, IMechE (London), 1965, 15-16.

[8] Dieter Steiner and Jerry Taborek, Flow boiling heat transfer in vertical tubes correlated by an asymptotic model, Heat Transfer Engineering 13 (2), 1992, 43-69.